

Exploring the Hydrogen Abstraction Pathway in HOM Formation from α -pinene Photooxidation Systems under Varying NO Conditions

Hui Wang^{1†}, Hongru Shen^{2†}, Defeng Zhao^{3,4*}, Sungah Kang¹, Rongrong Wu⁵, Yarê Baker⁶, Quanfu He⁷, Annika Zanders¹, Mathias Bachner⁸, Douglas R. Worsnop^{9,10}, Thorsten Hohaus¹, Thomas F. Mentel¹¹, Sören R. Zorn^{1*}

¹ Institute of Climate and Energy Research, ICE-3: Troposphere, Forschungszentrum Jülich, 52425 Jülich, Germany.

² School of Environmental Science and Engineering, Shanghai Jiao Tong University, Shanghai 200240, P. R. China

³ Shanghai Frontiers Science Center of Atmosphere-Ocean Interaction, Department of Atmospheric and Oceanic Sciences & Institute of Atmospheric Sciences, Fudan University, Shanghai 200438, China.

⁴ Institute of Eco-Chongming (IEC), 20 Cuinia Rd., Chongming, Shanghai, 202162, China.

⁵ Centre for Atmospheric Sciences, School of Earth, Atmospheric & Environmental Sciences, University of Manchester, M13 9PL Manchester, United Kingdom.

⁶ Leibniz Institute for Tropospheric Research (TROPOS), 04318 Leipzig, Germany

⁷ Earth, Ocean and Atmospheric Sciences (EOAS) Thrust, Function Hub, The Hong Kong University of Science and Technology (Guangzhou), 511458 Guangzhou, Guangdong, China

⁸ Institute of Technology and Engineering, Forschungszentrum Jülich, 52425 Jülich, Germany.

⁹ Institute for Atmospheric and Earth System Research/Physics, Faculty of Science, University of Helsinki, 00560 Helsinki, Finland.

¹⁰ Aerodyne Research, Inc., Billerica, 01821 Massachusetts, United States.

¹¹ Present Address: Keplerstrasse 13, 35390 Gießen, Germany

† These authors contributed equally to this work.

*Corresponding author.

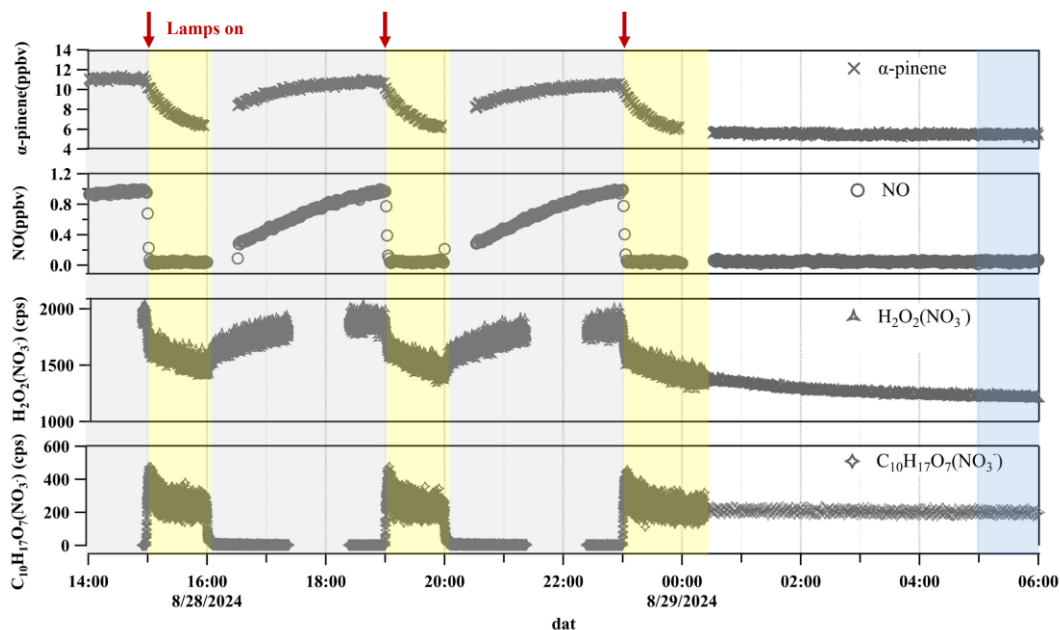


Figure S1. Time series of α -pinene concentration, NO concentration, along with normalized signal $\text{H}_2\text{O}_2(\text{NO}_3^-)$ and $\text{C}_{10}\text{H}_{17}\text{O}_7(\text{NO}_3^-)$. Three photooxidation experiments are presented, in which reactions were initialized by switching on UVC lamps when precursors are stable in dark conditions. In the third experiment, the lamps remain on for over six hours to allow the chamber to reach a steady-state condition.

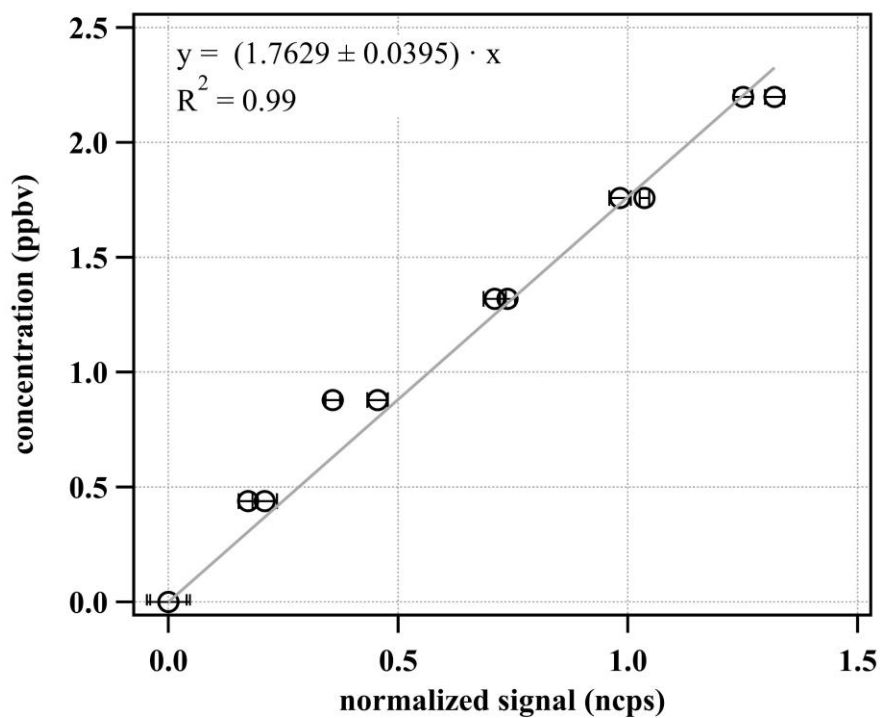


Figure S2. The calibration curve of pinonaldehyde in propylamine CIMS.

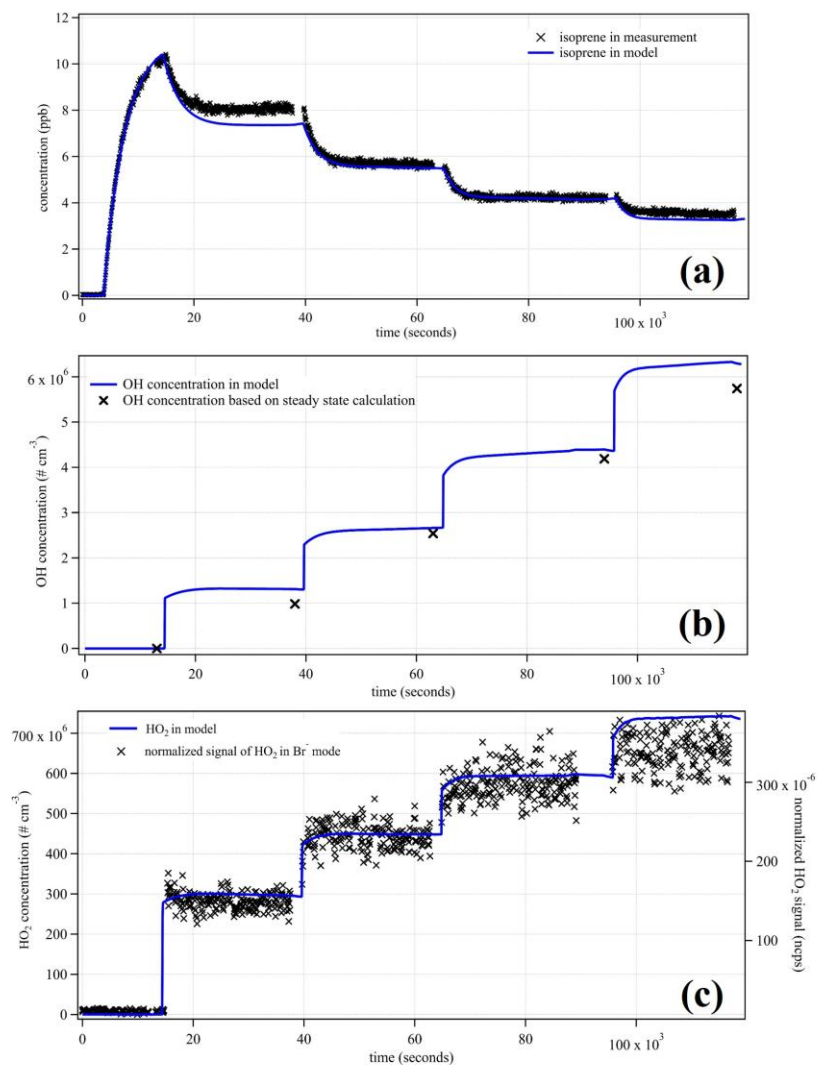


Figure S3. The time series of (a) measured isoprene (ppbv) and modeled isoprene (ppbv), (b) calculated concentration of $\cdot\text{OH}$ radicals and modeled $\cdot\text{OH}$ radicals, (c) normalized signal of $\text{HO}_2(\text{Br}^-)$ and HO_2 concentrations in model. The modeled data and measured data are presented in blue and dark, respectively.

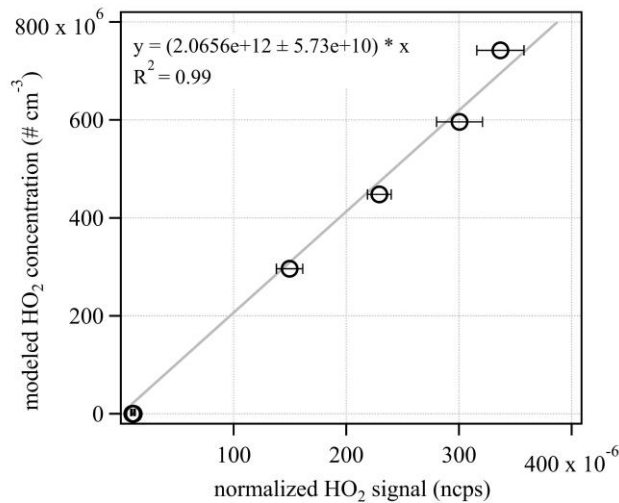


Figure S4. The modeled HO₂ concentrations are plotted versus normalized HO₂ signals, to obtain a calibration curve for HO₂ radicals.

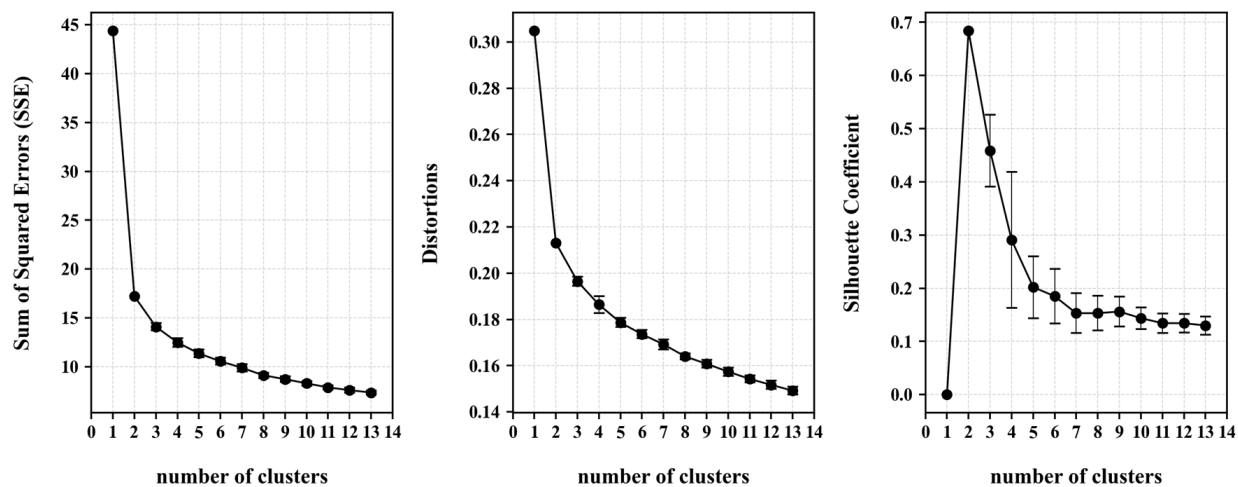


Figure S5. Values of selected clustering validity indices, sum of squared errors (SSE), distortions and Silhouette coefficients as a function of number of clusters from 1 to 13. The average of the results from 50 repetitions are shown in plots and error bars show the standard deviations.

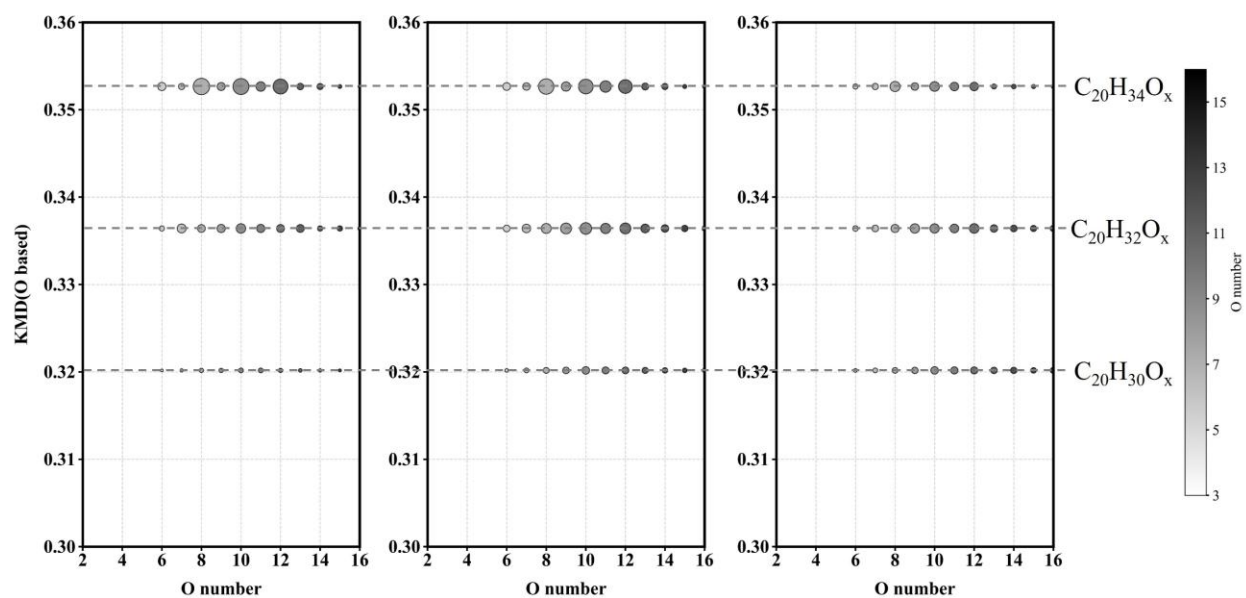


Figure S6. Kendrick Mass Defect (KMD, based on oxygen weight) of C_{20} accretion products as function of oxygen number are illustrated for without NO case (left), with low NO case (middle) and with high NO (right) case.

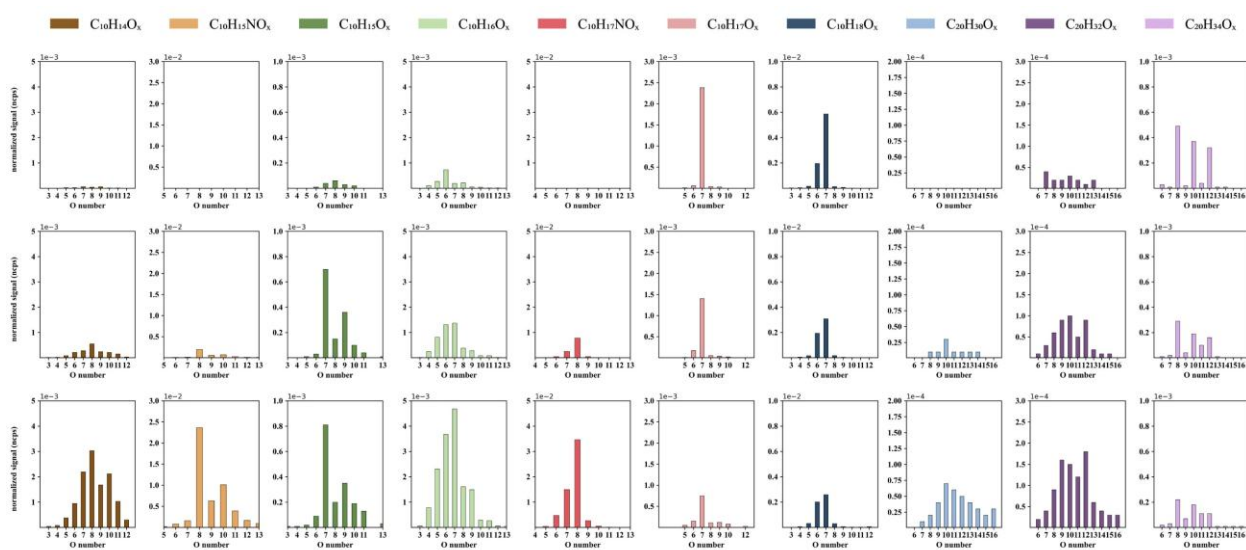


Figure S7. The normalized signals of major products are grouped into families are plotted versus oxygen number. From top to bottom, the three cases correspond to no-NO case, with low-NO case and with high-NO case, respectively. The data shown here are detected by nitrate CIMS.

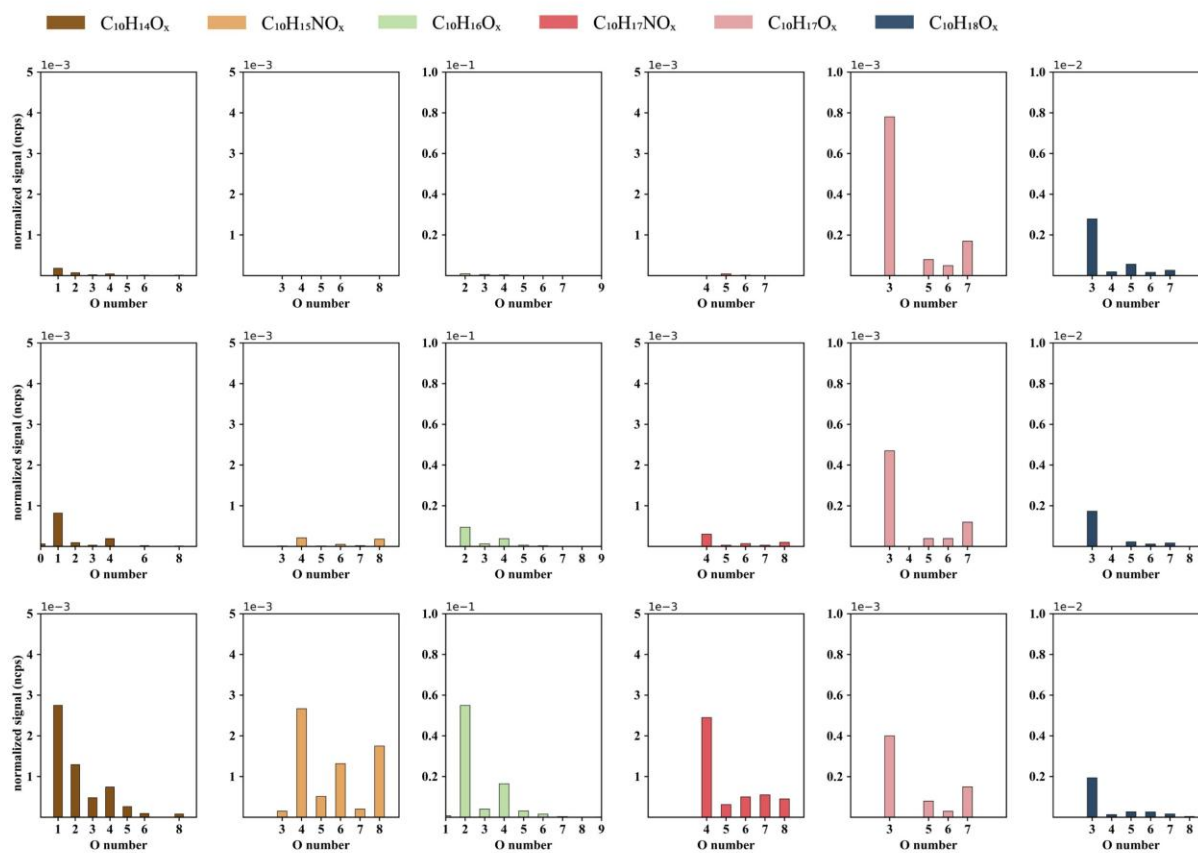


Figure S8. The normalized signals of major products are grouped into families and plotted versus oxygen number. From top to bottom, the three cases correspond to no-NO case, with low-NO case and with high-NO case, respectively. The data show only major monomers as measured by amine-CIMS.

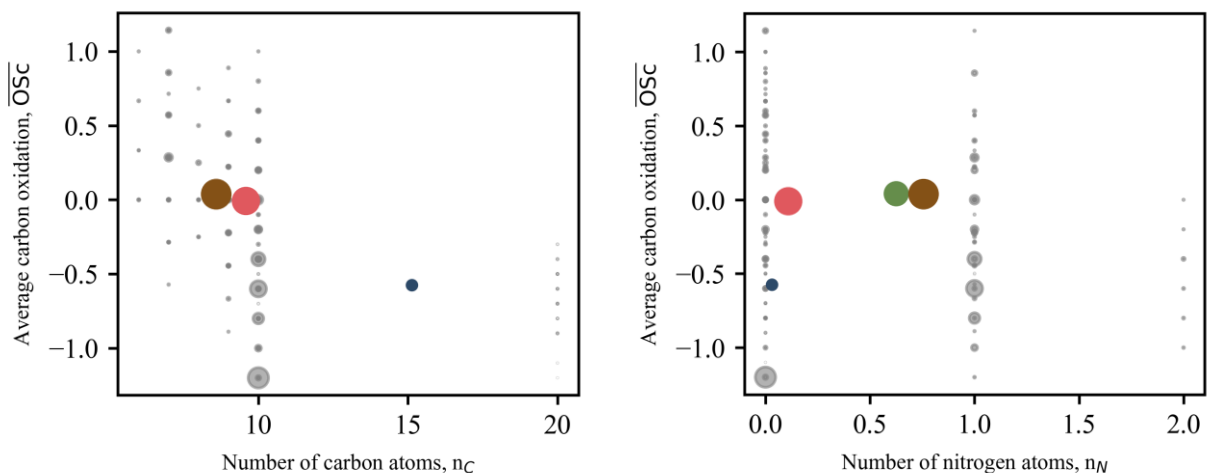


Figure S9. Average carbon oxidation state (\overline{OSc}) of four clusters obtained from fuzzy c-means clustering program are plotted as a function of average number of carbon atoms (left) and of average nitrogen atoms (right).

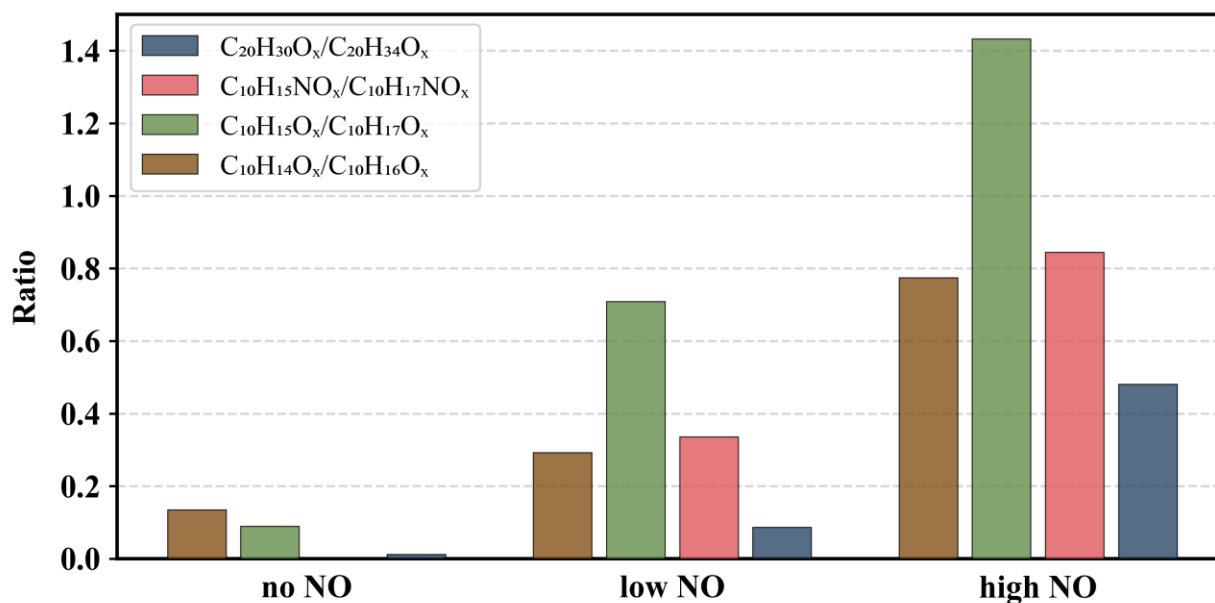


Figure S10. The bar plot represents ratios of product families potentially derived from H abstraction pathway to those potentially coming from $\cdot OH$ addition pathway.

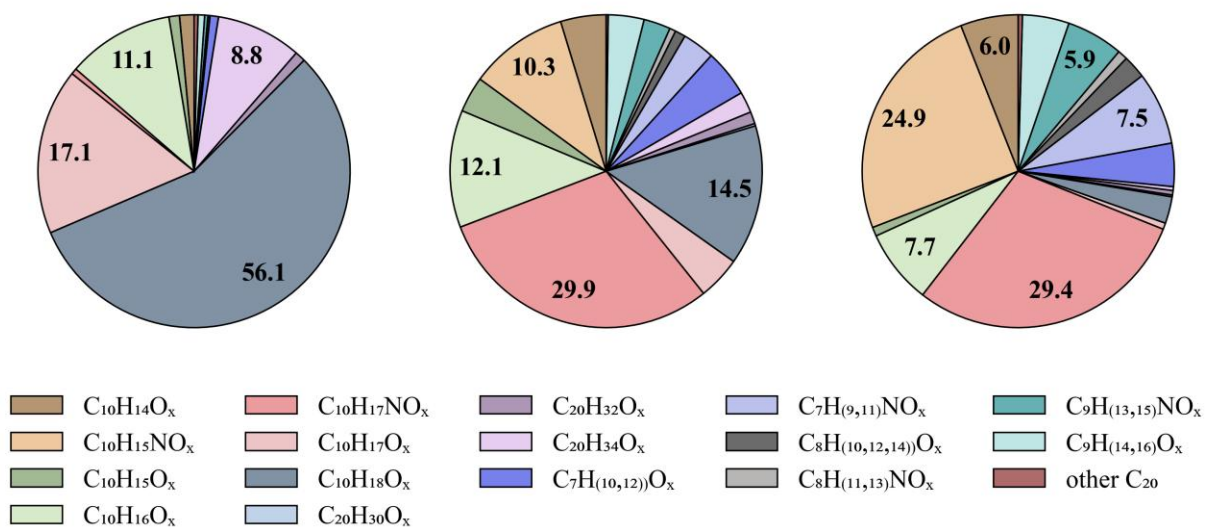


Figure S11. The pie plots illustrate the contribution of each family to the total compounds, from left to right showing no-NO case, with low-NO case and with high-NO case, respectively.